Available online at www.sciencedirect.com
SCIENCE DIRECT
ELSEVIER
Polymer 46 (2005) 7494–7503
polymer
www.elsevier.com/locate/polymer

Reaction pathways of superelectrophilic polycondensation of 2,2,2-trifluoroacetophenone and biphenyl. A computational study

Estrella Ramos Peña, Mikhail Zolotukhin, Serguei Fomine*

Instituto de Investigaciones en Materiales Universidad Nacional Autonoma de Mexico, Apartado Postal 70-360, CU, Coyoacan, Mexico DF 04510, México

Received 8 April 2005; received in revised form 25 May 2005; accepted 26 May 2005
Available online 1 July 2005

Abstract

For the first time possible reaction pathways of superelectrophilic polycondensation of 2,2,2-trifluoroacetophenone and biphenyl in trifluoromethanesulfonic acid (TSFA) have been studied theoretically at B3LYP/aug-cc-pvtz(-f)//B3LYP/6-31G* level. The reaction graph reveals the existence of four different reaction routes for polycondensation process. The analysis of the reaction pathways shows that kinetically most favorable pathway involves the successive reaction between protonated 2,2,2-trifluoroacetophenone and neutral oligomers. The reactivity indexes best correlated with calculated thermodynamic and kinetic parameters are these based on the energy difference between the ionization potential of a nucleophile and the electron affinity of a electrophile showing correlation coefficients up to 0.95. These reactivity indexes can be successfully used for the prediction of the most favorable reaction pathways in the superelectrophilic polycondensation. The calculations established basic rules for efficient design of monomers for superelectrophilic polycondensation.

Keywords: Superelectrophilic polymerization; B3LYP calculations; 2,2,2-trifluoroacetophenone

1. Introduction

There has been considerable interest over last two decades in the preparation of aromatic fluorine-containing polymers due to their unique properties and high-temperature performance. The incorporation of fluorine atoms (or groups containing fluorine atoms) into macromolecules leads to polymers with increased solubility, glass transitions temperature, thermal stability and chemical resistance, while also leading to decreased moisture uptake, dielectric constant and colour [1].

In many cases fluoro-containing monomers are very expensive, and few of them are commercially available. Clearly, simple, reliable syntheses of aromatic fluorine-containing polymers combined with the minimum number of reaction steps would be of great importance.

In this respect, the theory of superelectrophilic activation, suggested by Olah to explain high reactivity of some electrophiles in superacid solutions, presents a promising challenge [2].

Recently, using this approach, we reported the first preparation of linear, high-molecular-weight polymers by reaction of 2,2,2-trifluoroacetophenone with non-activated aromatic hydrocarbons using TFSA as a solvent–catalyst [3]. Simple, practical, metal-free, one-pot preparation opens up wide possibilities for constructing of new polymers using cheap, commercially available monomers. It is also important that, according to characterization data, and, particularly, their low melt viscosity, the polymers are promising candidates for high performance engineering plastics. For example, 2,2,2-trifluoroacetophenone reacts even with different aromatic molecules under these conditions to give high molecular weight film forming polymer:

* Corresponding author.
E-mail address: fomine@servidor.unam.mx (S. Fomine).

0032-3861/$ - see front matter © 2005 Elsevier Ltd. All rights reserved.
doi:10.1016/j.polymer.2005.05.139

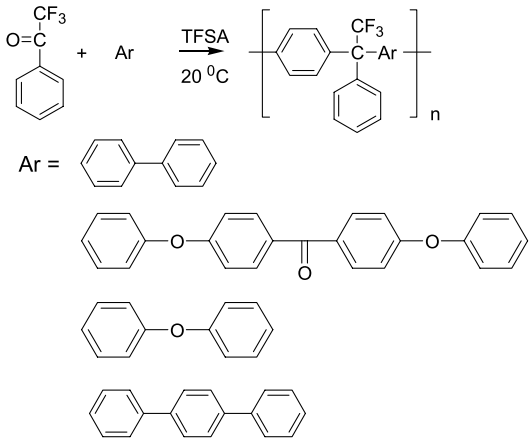

In a further exploration of the scope of polymer-forming reactions of 2,2,2-trifluoroacetophenone with aromatic hydrocarbons catalyzed by superacids we carried out a theoretical study of the mechanism of elemental steps of C–C forming reaction in superelectrophilic polycondensation involving carbonyl compounds bearing electron-withdrawing groups, adjacent or relatively close to a carbocation center. It was established [4] that the introduction of electron-withdrawing groups into the carbonyl compound reduces activation and total reaction energies of the aromatic electrophilic substitution reaction. The enhancement of the reactivity of carbonyl compounds bearing electron-withdrawing groups is due to lowering of LUMO energy. The electrophiles having highly delocalized LUMO are less active in the reaction of electrophilic aromatic substitution due to decreases of local LUMO density at the reaction center.

Although, the mechanism of elemental steps of C–C forming reaction in superelectrophilic polycondensation has been documented [4] there is another important unsolved problem. What is the particular reaction pathway from monomers to polymer during the polycondensation? This point is extremely important since there are multiple reaction pathways from monomers to polymer in case of superelectriphilic polycondensation.

Therefore, the aim of the present work is to study possible reaction pathways for TFSA catalyzed polycondensation between 2,2,2-Trifluoroacetophenone and biphenyl in TFSA medium using quantum chemistry tools to obtain deeper insight into the reaction mechanism of superelectrophilic polycondensation and develop basic knowledge for the design of monomers for superelectrophilic polycondensation.

2. Computational details

All calculations were carried out with Jaguar v 5.5 program [5]. The geometry optimizations were run using hybrid B3LYP functional without any symmetry restrictions at B3LYP/6-31G* level of theory which is successful for modeling of organic molecules [6]. Frequency calculations were run for all structures at the same level of theory to make sure that a transition state (one imaginary mode) or minimum (zero imaginary modes) is located and to reach zero point energy (ZPE) correction and thermodynamic properties. Poisson–Boltzman solver [7,8] as implemented in Jaguar v 5.5 was used to calculate the solvation effects on the studied molecules in TFSA at B3LYP/aug-cc-PVTZ(-f) level of theory. In other words, the structures have not been reoptimized in the presence of solvent since it has been shown previously that reoptimization has very limited effect on the computed energies [9–12].

Vertical ionization potentials (IPs), electron affinities (AE), global electrophilicity (ω) indexes and local Fukui functions (f) of the reaction intermediates were calculated at B3LYP/6-31G* level of theory. IPs and AEs were obtained as $E_{n-1}-E_n$ and E_n-E_{n+1}, respectively, where E_n is the total electronic energy of n-electron system and E_{n-1} and E_{n+1} are the energies of systems with $n-1$ and $n+1$ electrons. ω was calculated according to Ref. [13] as $\mu^2/2\eta$, where μ is chemical potential approximated as $-(\mathrm{IP}+\mathrm{AE})/2$ and η is chemical hardness approached as $(\mathrm{IP}-\mathrm{AE})$. The Fukui local function at site for electrophilic and nucleophilic agents, were approached by the gross natural charge (q) at site k, (k=atom) for systems with $n-1$, and $n+1$ electrons, respectively, where n is the number of electrons in studied species as $f_k^+ = q_k(n+1) - q_k(n)$ and $f_k = q_k(n) - q_k(n-1)$ [14].

3. Results and discussions

3.1. Reaction paths

It has been shown [15], that under superacid conditions diprotonated species are responsible for the unusually high reactivity of carbonyl-containing molecules toward some of aromatic hydrocarbons. Therefore, it seems that diprotonated carbonyl species are of importance for the reactions under consideration. However, the experimental data show [3] that it is the presence of electron-withdrawing group attached to carbonyl fragment that makes the polycondensation possible. Eventually, diprotonation could hardly have to do with acceleration of polycondensation under superacid conditions since electron withdrawing groups reduces the protonation equilibrium constant and, therefore, monoprotonated carbonyl component **1** was considered to be correct approximation for the electrophilic species participating in the polycondensation. Since the reaction is carried out in TFSA solution it is reasonably to suggest that TFSA anion is responsible for deprotonation of aromatic species during the reaction cycle.

The reaction of aromatic electrophilic substitution has been a subject of intensive theoretical studies [16–18]. It is well established that, the reaction steps involves the complex formation between the electrophile and aromatic

hydrocarbon which is transformed into the σ intermediate. The σ intermediate looses proton to recover the aromaticity. It is suggested that the rate determining step is the formation of the σ intermediate [19], therefore, the transition state search was carried out only for the formation of σ intermediate to save computational time. The π-adduct formation previous to the formation of the σ intermediate was not taken into account by following reasons:

1. The formation of weak complexes is governed by dispersion interactions which are described incorrectly by modern DFT theory [20]. The high level theories correctly describing dispersion interactions are prohibitive due to size of the treated molecules.
2. The available calculated binding energies for π-adducts for the reaction of proton exchange and methylation of benzene are not exceeded 4 kcal/mol [18]. Moreover, when comparing the difference of activation energies, the formation of π-adducts will be affecting even less the energetic due partial compensation effect.

The different reaction paths for the polycondensation of biphenyl and 2,2,2-trifluoroacetophenone are shown in Schemes 1–4. The target oligomer in all cases is compound **14**. There are four different reaction pathways to reach molecule **14**. As seen from the Scheme 1 the first reaction pathway is a consecutive reactions of growing neutral polymer chain with protonated 2,2,2-trifluoroacetophenone **1**. The second reaction pathway which is presented in Scheme 2 follows Scheme 1 until the formation of carbocation **5**, which then attacks biphenyl to give neutral molecule **8**, again followed by the reaction with carbocation **5** to give target molecule **14**. The third reaction route (Scheme 3) follows Schemes 1 and 2 until the formation of intermediate **5**. The dimerization of carbocation **5** affords dication **22** which is transformed into cation **11** on deprotonation following by the reaction with biphenyl to form target oligomer **14**. The forth reaction route (Scheme 4) involves the reaction of intermediate **5** with protonated 2,2,2-trifluoroacetophenone **1** affording dication **19** which reacts successively with two molecules of biphenyl giving oligomer **14**.

Since the starting and the final points are the same for all routes there is no difference between four different reaction paths from the thermodynamic point of view. To find the most favorable reaction path out of four possible reaction routes one needs to locate the route with lowest activation energy at branching points. Fig. 1 shows the graph of the reaction routes. As seen from the Fig. 1 there are two branching points on the graph. One corresponds to the reaction of intermediate **5** (triple branching) another—to the reaction of intermediate **8** (double branching).

Tables 1 and 5 show solution phase electronic and the free Gibbs reaction energies and total electronic and the free Gibbs energies of the intermediates involved into the reactions Schemes 1–4, respectively. Fig. 3 shows optimized geometries of all located transition states. As seen the most favorable reaction path from intermediate **5** among three possible (**5**+**1**=**18**. **5**+**5**=**22** and **5**+**2**=**6**) is the last reaction. Both the activation energy and the activation free Gibbs energy are the most favorable for the reaction step **5**+**2**=**6**. The same situation holds for the reaction and the free Gibbs reaction energies which are most favorable for the reaction **5**+**2**=**6**. Therefore, one can discard reaction paths showed in Schemes 3 and 4 as possible reactions routes for the polycondensation of monomers **1** and **2**. As seen from the Fig. 1 there is another branching point on the way from **1** to **14** which is intermediate **8**. Since routes 3 and 4 were discarded the only possible ways to final product **14** are routes 1 and 2 (Schemes 1 and 2, respectively). The first one is **8**−**11**−**14** and the second one is **8**−**16**−**14**. The first step for the route 1 is the reaction **8**+**1**=**10** and the first reaction step for route 2 is the reaction **8**+**5**=**16**. As seen from the Table 1 the first route is favored both, thermodynamically and kinetically. Therefore, according to the analysis the most favorable reaction path from the kinetic point of view conducting from monomers **1** and **2** to oligomer **14** is the reaction path 1 (Scheme 1). All other reaction routes can be ordered in descending order according to their accessibility as route 2 route 4 and route 3. It is noteworthy that in case of route 4 no transition state has been detected for the reaction **1**+**5**=**18**, and only total reaction energies or the free Gibbs energies are available. However, we believe, that according to the Hammond postulate [21], the structure and the energy of the transition state for the reaction **1**+**5**=**18** must be close to intermediate **18** (the situation which holds for the reaction **5**+**5**=**22**).

To predict with certainty the most favorable reaction path one needs to examine the whole energetic profile of the reaction routes. (Fig. 2) shows energy profiles for four possible reaction routes at B3LYP/aug-cc-pvtz(-f)//B3LYP/6-31G* level of theory. As seen from the profiles in all cases the branching points in the reaction paths correspond to the highest activation energies on the reaction paths. The energy profile for the free Gibbs energies is very similar.

The reaction route most favored from the kinetic point of view is route 1 consisting in the reaction of neutral molecules with electrophile **1**. The difference between routes 1 and 2 is the reaction of **8** with cation **1** (route 1) and with intermediate **5** (route 2). The difference between route 1 and 3 is the dimerization of cation **5** instead of the reaction of with **2**. The route 4 implies the reaction of **5** with **1** at the branching point. Therefore, the understanding of the reactivity of the reaction intermediates can be achieved using reactivity indexes of the key intermediates.

3.2. Reactivity indexes

Table 2 shows various reactivity indexes calculated for selected reaction intermediates. It is interesting to test whether is possible to predict kinetically most favorable

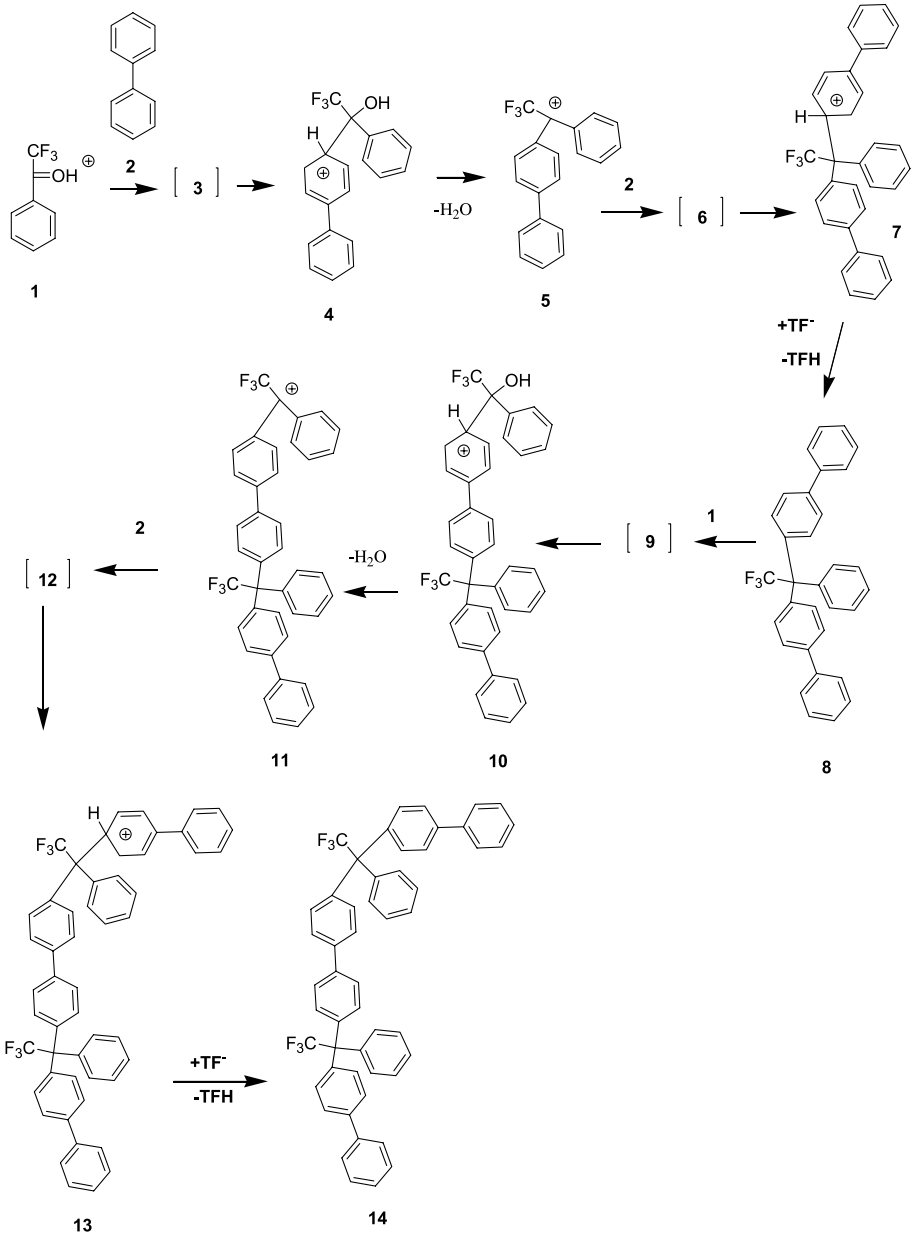

Scheme 1. Reaction route 1. Intermediates in brackets are transition states.

reaction pathway without laborious calculations of the reaction paths. Thus, at fist branching point (Fig. 1) one need to distinguish between three reactions: **5**+**2** (route 1) **5**+**5** (route 3) and **5**+**1** (route 4). In the first reaction cation **5** is an electophile, in second one cation **5** is an electrophile and a nucleophile at the same time and in the last case cation **5** is an nucleophile. The most straightforward way is to compare the energy difference between LUMO of electrophile and HOMO of nucleophile since aromatic molecules are soft electrophiles and nucleophiles and reactions between them are orbitally controlled. The best approximation to HOMO and LUMO energies is IP and AE, respectively. Using data from the Table 2 one can obtain IP−AE difference of 0.06533, 0.192199 and 0.185649 a.u., for routes 1, 3 and 4, respectively. As seen, smallest IP−AE difference corresponds to lower activation reaction energy (**5**+**2**, route 1). Next branching point is intermediate **8** where one needs to distinguish between reactions **8**+**1** (route 1) and **8**+**5** (route 2) where **8** is a nucleophile and **5** is an electrophile. The IP−AE difference for those reactions is 0.03733 and 0.04388 a.u. which is in accordance with activation energies (lowest for **8**+**1** reaction).

Therefore, the IP−AE difference of nucleophile and electrophile allows us to predict the most favorable reaction path without doing sophisticated calculation. It is interesting to compare the performance of this reaction index for other studied reactions as well as to compare the performance of other commonly accepted electrophilicity indexes for the

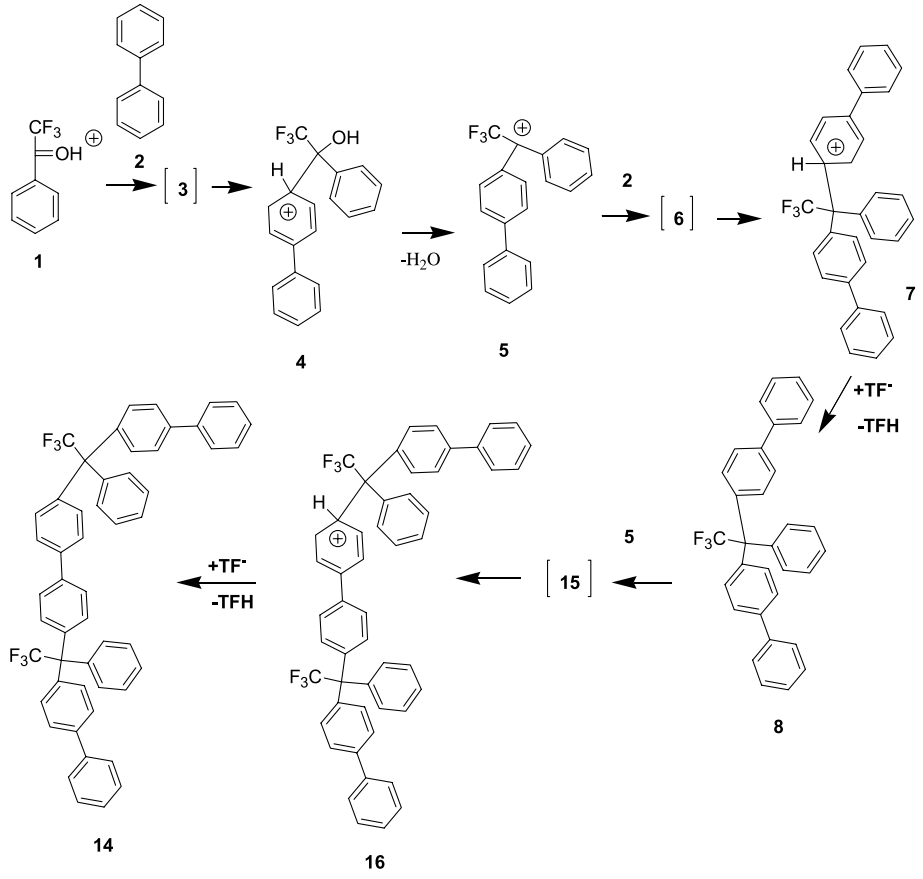

Scheme 2. Reaction route 2. Intermediates in brackets are transition states.

reactions of interest. Table 2 shows the reactivity indexes calculated for reaction intermediates such as local nucleophilic (f^-) and electropholic (f^-) Fukui functions, global (ω) lectrophilicities, AE, IP for electrophiles and two nucleophiles participating in the polymerization process. Table 3 shows (IP−AE), $(P-A)/(f^+)(f^-)$ and $\Delta\omega$ indexes; the last represents the difference between global electrophilicites of electrophile and nucleophile participating in the reaction of σ-complexes formation along with calculated thermodynamic and kinetic data of the reactions. Table 4 presents the linear fit correlation coefficients calculated between activation (E_a), total electronic (ΔE),

Table 1
Reaction and activation energies (kcal/mol) and the free Gibbs energies calculated at B3LYP/aug-cc-pvtz(-f)//B3LYP/6-31G* and B3LYP/6-31G*//B3LYP/6-31G* levels of theory, respectively, in TFSA solution

Reaction	ΔG	G_a	ΔE	E_a
1+2=[3]=4	21.7	25.0	12.2	16.2
4=5+H_2O	−18.6	–	−18.9	–
5+5=[17]=22	37.7	44.0	28.4	34.2
5+2=[6]=7	28.0	33.4	19.3	24.4
22+TF^-=11+TFH	−25.9	–	−26.4	–
7+TF^-=8+TFH	−18.7	–	−18.1	–
8+1=[9]=10	23.1	27.8	12.7	17.2
10=11+H_2O	−17.5	–	−18.6	–
11+2=[12]=13	20.3	32.6	12.6	23.4
8+5=[15]=16	26.8	35.1	15.7	23.8
16+TF^-=14+TFH	−13.0		−12.4	
13+TF^-=14+TFH	−8.9	–	−10.1	–
5+1=18	35.2	–	26.1	–
18=19+H_2O	−21.6	–	−22.6	–
19+2=[20]=21	16.9	27.6	6.5	16.8
21+TF^-=11+TFH	−15.6	–	−14.8	–

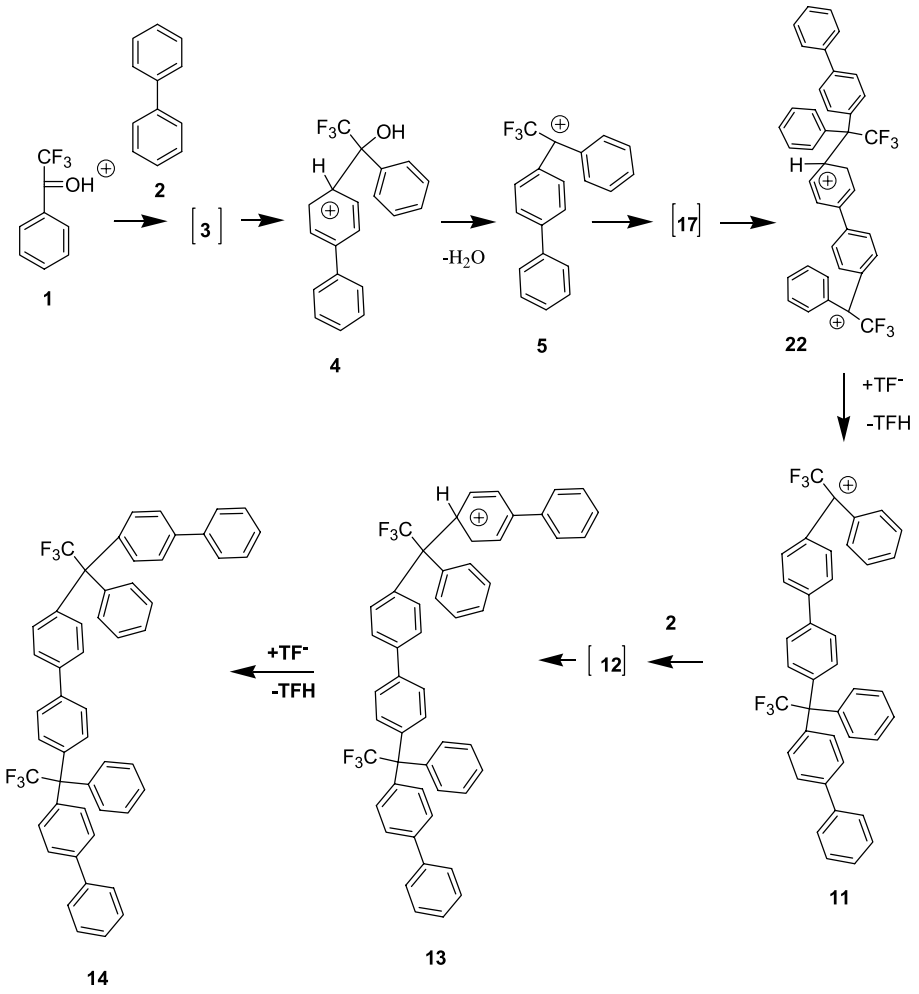

Scheme 3. Reaction route 3. Intermediates in brackets are transition states.

the free Gibbs activation (G_a), the free Gibbs reaction energies (ΔG) and the corresponding reactive indexes listed in the Tables 2 and 3 fitting a line to the data.

The correlation coefficients for AE and ω were calculated for the reaction of four different electrophiles (**1**, **5**, **11** and **19**) with biphenyl (**2**) while for the calculations of the correlation coefficients for IP − AE, $(IP-A)/(f^+)(f^-)$ and $\Delta\omega$ were used data from the Table 3.

One can make various conclusions inspecting Table 4. The first one is that calculated reactive indexes correlate better with thermodynamic parameters rather than with kinetic ones. Second, the correlation coefficients are similar for the data obtained on the basis of the total electronic energies and the free Gibbs energy showing no clear preference for one of them (Table 5). Third, simple electron affinity shows almost the same correlation coefficient with reaction and activation energies as more sophisticated global electrophilicity index, at least for studied systems. Forth, using local quantities instead of global ones has little effect on the correlation coefficients. Fifth and the last, complex correlation indexes including both an electrophile and a nucleophile information show best correlation with reaction and activation energies. The best performance show complex index based on the difference of IP and AE as

Table 2
Vertical ionization potentials (IP), electron affinities (AE), global electrophilisity indexes (ω) (a.u.) and local electrophilic (f^+) and nucleophilic (f^-) Fukui functions (e) for selected reaction intermediates calculated at B3LYP/6-31G*//B3LYP/6-31G* level of theory

	IP	AE	ω	f^+	f^-
5	0.414389	0.22219	0.26355	0.15816	0.13324
1	0.52051	0.22874	0.24051	0.23442	–
11	0.33784	0.21993	0.32983	0.15085	–
19	0.50593	0.32346	0.47124	0.105315	–
2	0.28752	−0.03877	0.02370	0.12491	0.13491
8	0.26607	−0.01134	0.02924	0.06069	0.068995

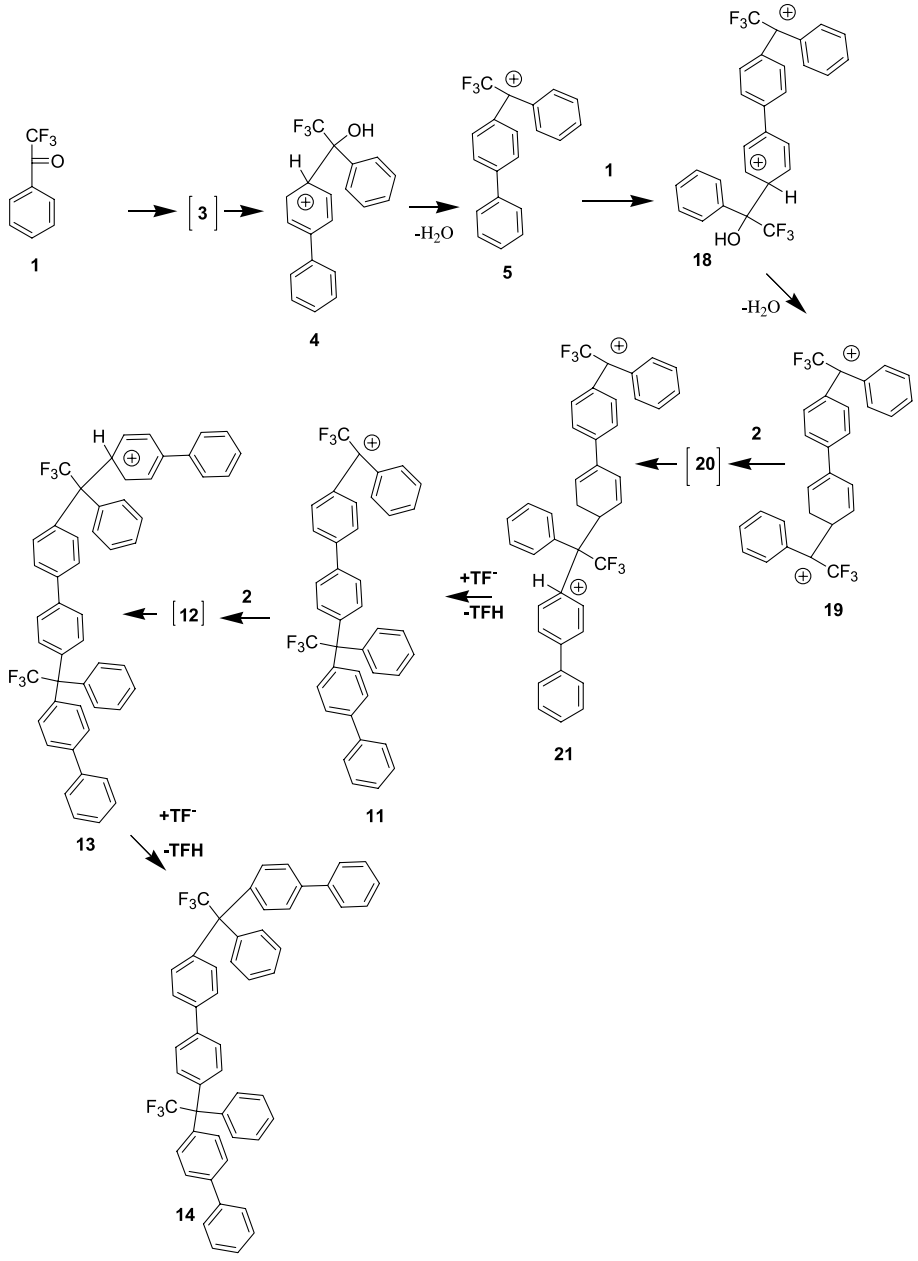

Scheme 4. Reaction route 4. Intermediates in brackets are transition states.

Table 3
Complex reactive indexes for selected reactions calculated at B3LYP/6-31G*//B3LYP/6-31G* level of theory

Reaction	IP−AE	(IP−A)/(f^+)(f^-)	$\Delta\omega$
5+**5**=[**17**]=**22**	0.192199	9.12053	0
5+**2**=[**6**]=**7**	0.06533	3.06177	0.23985
5+**1**=**18**	0.185649	5.94379	0.02304
8+**1**=[**9**]=**10**	0.03733	2.30805	0.21127
8+**5**=[**15**]=**16**	0.04388	4.02117	0.23431
1+**2**=[**3**]=**4**	0.05878	1.85862	0.21681
11+**2**=[**12**]=**13**	0.06759	3.32118	0.30613
19+**2**=[**20**]=**21**	−0.03594	−2.52955	0.44754

IP (a.u) and f^- (e) were calculated for nucleophile and AE (a.u) and f^+ (e) for electrophile. $\Delta\omega$ is the difference of global electrophilicities of an electrophile and a nucleophile.

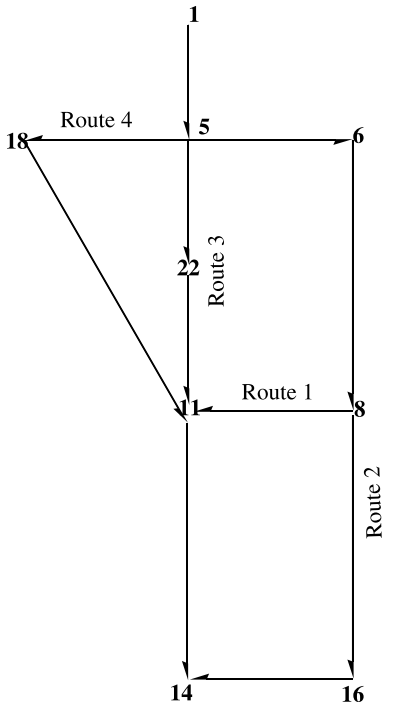

Fig. 1. Reaction graph for possible reaction routes.

Table 4
Correlation coefficients between calculated reactivity indexes and thermodynamic and kinetics parameters of studied reactions

Reactivity index	E_a	ΔE	G_a	ΔG
AE	0.58	0.80	0.29	0.70
ω	0.30	0.78	0.57	0.76
IP−AE	0.86	0.95	0.80	0.92
(IP−A)/(f^+)(f^-)	0.88	0.92	0.86	0.91
$\Delta\omega$	0.72	0.93	0.69	0.93

well as their local analogue (Table 4) showing correlation coefficients in the range of 0.85–0.95 for all calculated reaction and activation energies. Therefore, IP−AE difference between nucleophile and electrophile, respectively, can be successfully used for the predictional purpose in the reactions of superelectriphilic polycondensation.

4. Conclusions

According to calculations kinetically most favorable reaction pathway is one involving the reaction of protonated 2,2,2-trifluoroacetophenone and growing neutral oligomer (Scheme 1). This situation, however, is only possible at the beginning of the polycondensation process when monomer

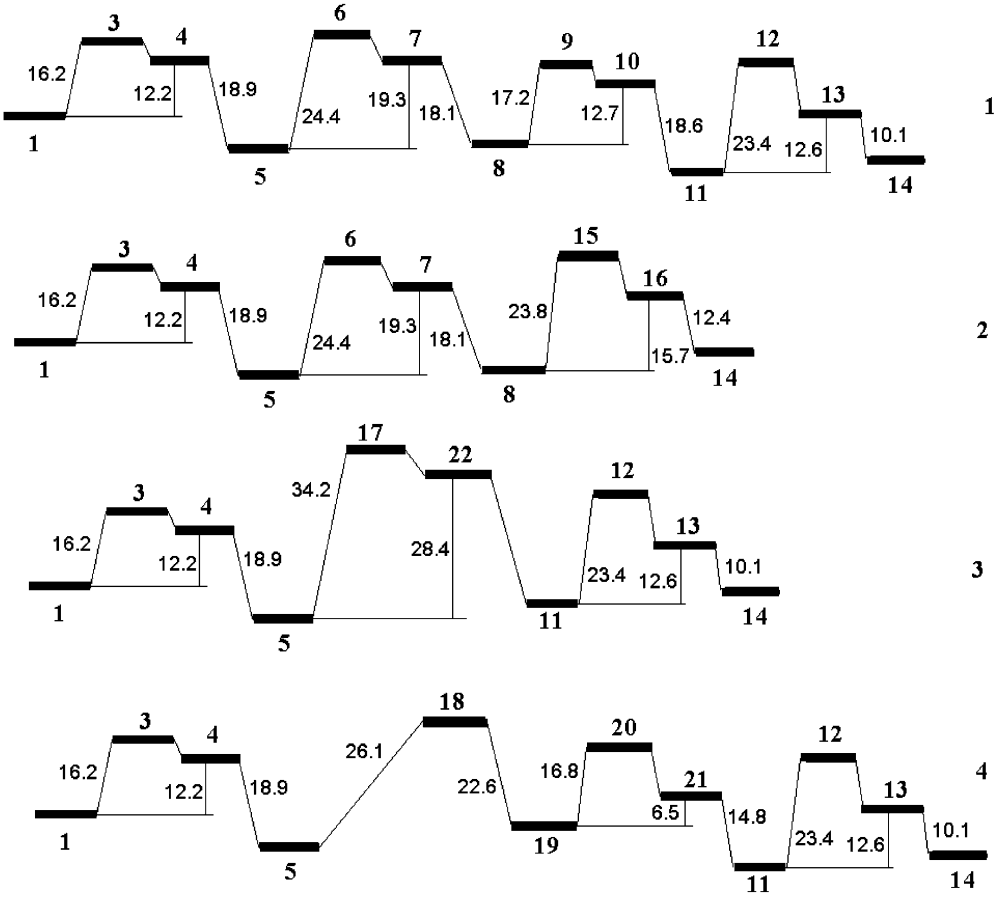

Fig. 2. Reaction energies (kcal/mol) for four different reaction paths calculated at B3LYP/aug-cc-pvtz(-f)//B3LYP/6-31G* level of theory in TFSA solution.

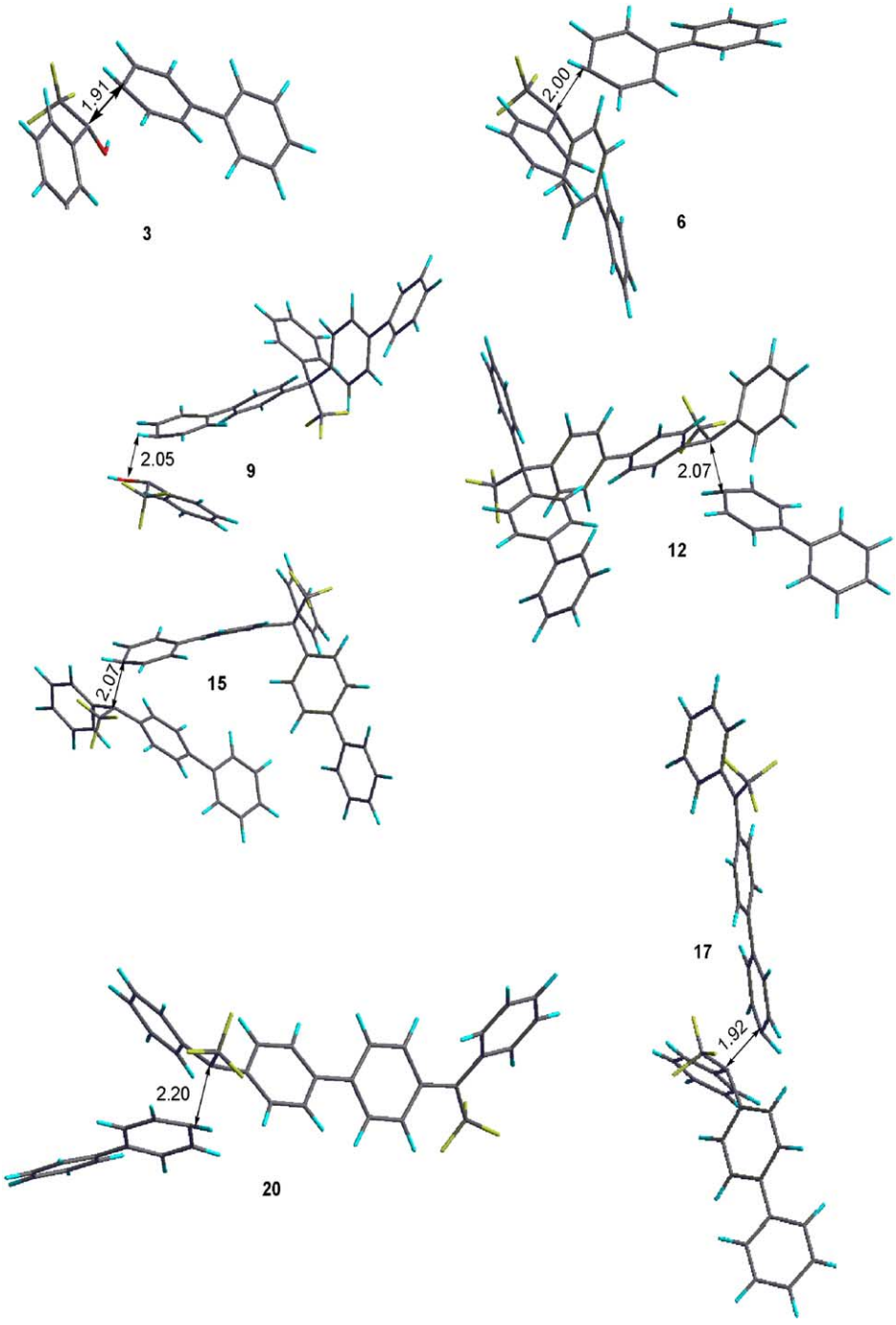

Fig. 3. Molecular geometries of transition states optimized at B3LYP/6-31G* level of theory.

concentration is still high in the reaction mixture. At the latter polymerization stages the most probable reaction pathway becomes the route 2 (Scheme 2) where neutral oligomer molecules react with a macrocation. The reactions between two cationes (routes 3 and 4) Schemes 3 and 4 are prohibitive due to high activation energies. Among different reactivity indexes tested to predict the most favorable reaction paths the most effective are these based on the difference between IP and EA on nucleophile and electrophile, respectively, showing the correlation coefficient up to 0.95 with reaction and activation energies. This results can be understood in terms of orbital interactions. The difference between IP and EA is approximated by HOMO–LUMO energy difference. Therefore, the smaller HOMO–LUMO difference the stronger orbital interactions decreasing the reaction activation energy. The calculations established basic rules for efficient design of monomers for superelectrophilic polycondensation.

Table 5
ZPE corrected total electronic (*E*) and the free Gibbs energies (*G*) of calculated intermediates in TSFA solution at B3LYP/aug-cc-pvtz(-f) //B3LYP/6-31G* and B3LYP/6-31G*//B3LYP/6-31G* levels of theory, respectively, in a.u.

Intermediate	*E*	*G*
1	−683.133107	−682.9246995
2	−463.275997	−463.1659037
3	−1146.383348	−1146.050847
4	−1146.389646	−1146.055998
5	−1069.962916	−1069.665965
6	−1533.199970	−1532.778711
7	−1533.208151	−1532.787248
8	−1532.844918	−1532.41616
9	−2215.950637	−2215.296553
10	−2216.309096	−2215.665756
11	−2139.530576	−2138.912358
12	−2602.769302	−2602.026255
13	−2602.786482	−2602.045928
14	−2602.410367	−2601.659325
15	−2602.769934	−2602.026123
16	−2602.782806	−2602.039391
17	−2139.871335	−2139.261822
18	−1753.054361	−1752.534541
19	−1676.633528	−1676.149309
20	−2139.882698	−2139.271217
21	−2139.899091	−2139.288238
22	−2139.871335	−2139.261822
TF	−1037.517690	−1037.234804
TF^-	−1037.125542	−1036.83399
Water	−76.456858	−76.41962954

Acknowledgements

Authors thank DGAPA (project PAPIIT IN101405-3) for support.

References

[1] (a) Harris FW, Hsu SLC. High Perform Polym 1989;1:3.
(b) Cassidy PE, Aminabhavi TM, Fartley JM. J Macromol Sci Rev, Macromol Chem Phys 1989;29:365.
(c) Goodwin AA, Mercer FW, McKenzie MT. Macromolecules 1997;30:2767.
(d) Hellums MW, Koros WJ, Husk GR, Paul DR. J Membr Sci 1989; 46:93.
(e) Ghosal K, Freeman BD. Polym Adv Technol 1994;5:673.
(f) Banerjee S, Maier G. Chem Mater 1999;11:2179.
(g) Maier G. Prog Polym Sci 2001;26:3.
(h) Liu BJ, Hu W, Chen CH, Jiang ZH, Zhang WJ, Wu ZW. Polym Adv Technol 2003;14:221.
(i) Simone CD, Scola DA. Macromolecules 2003;36:6780.
(j) Kim S-U, Lee C, Sundar S, Jang W, Yang S-J, Han H. J Polym Sci, Part B: Polym Phys 2004;42:4303.
[2] Olah GA. Angew Chem, Int Ed Engl 1993;32:767.
[3] Zolotukhin MG, Fomine S, Salcedo R, Khalilov L. Chem Commun 2004;1030.
[4] Ramos Peña E, Zolotukhin M, Fomine S. Macromolecules 2004;37: 6227.
[5] Jaguar 5.5. Schrodinger, LLC, Portland, Oregon; 2003.
[6] Foresman JB, Frisch A. Exploring chemistry with electronic structure methods. Pittsburgh, PA: Gaussian, Inc.; 1996.
[7] Tannor DJ, Marten B, Murphy R, Friesner RA, Sitkoff D, Nicholls A, et al. J Am Chem Soc 1994;116:11875.
[8] Marten B, Kim K, Cortis C, Friesner RA, Murphy RB, Ringnalda MN, et al. J Phys Chem 1996;100:11775.
[9] Barone V, Cossi M, Tomasi J. J Chem Phys 1997;107:3210.
[9] Pomeli CS, Tomasi J, Sola M. Organometallics 1998;17:3164.
[10] Cacelli I, Ferretti A. J Chem Phys 1998;109:8583.
[11] Creve S, Oevering H, Coussens BB. Organometallics 1999;18:1907.
[12] Bernardi F, Bottoni A, Miscone GP. Organometallics 1998;17:16.
[13] Parr RG, Szentpály LV, Liu S. J Am Chem Soc 1999;121:1922.
[14] Yang W, Mortier WJ. J Am Chem Soc 1986;108:5708.
[15] Saito S, Ohwada T, Shudo K. J Am Chem Soc 1995;117:11081.
[16] Esteves PM, de M Carneiro JW, Cardoso SP, Barbosa AGH, Laali KK, Rasul G, et al. J Am Chem Soc 2003;125:4836.
[17] Szabo KJ, Hornfeldt AB, Gronowitz S. J Am Chem Soc 1992;114: 6827.
[18] Vos AM, Schoonheydt RA, De Proft F, Geerlings P. J Catal 2003;220: 333.
[19] Solomons TWG. Fundamentals of organic chemistry. 5th ed. New York: Wiley; 1997.
[20] Chalasinski G, Szczesniak MM. Chem Rev 2000;100:4227.
[21] Hammond GS. J Am Chem Soc 1955;77:334.